

CNN-BiLSTM hybrid neural networks with attention mechanism for well log prediction

Liqun Shan^{a,*}, Yanchang Liu^a, Min Tang^a, Ming Yang^b, Xueyuan Bai^a

^a Northeast Petroleum University, Daqing, China

^b Westfield State University, Westfield, USA



ARTICLE INFO

Keywords:

Well logs
CNN
BiLSTM
Attention mechanism
Prediction

ABSTRACT

Well logging is a significant method of formation description and resource assessment in exploration and development of oil, natural gas, minerals, groundwater, and sub-surface thermal energy, as well as geotechnical engineering and environmental research. However, the shortage problem of well logging data always exists because well logs can only be measured through a drilling process involving costly and time-consuming field trials. To address this issue, bidirectional long short-term memory (BiLSTM), attention mechanism, and convolutional neural network (CNN) were coupled to build hybrid neural networks for predicting missing well logs. The proposed architecture is a structure of two branches. One branch uses CNN to capture the spatial properties of well logs, and the other one conducts the feature selections by utilizing two-layer BiLSTM with attention mechanism. The spatio-temporal correlations from two branches are merged to forecast the target well logs. The performance of the proposed method is evaluated within a highly heterogeneous reservoir at the Gangdong oilfield in China. In our experiments, six models were trained and used for generating synthetic well logs including compensated neutron logs (CNL), acoustic (AC), spontaneous potential (SP), gamma-ray (GR), density (DEN), and formation resistivity (RT). Moreover, traditional machine learning models, CNN, BiLSTM, and other deep learning benchmark models were developed to compare with the presented models. Results show that the proposed method achieves higher prediction accuracy because it takes into account the spatio-temporal information of well logs.

1. Introduction

Well logging records the practice of the geologic formations along a borehole (Avseth et al., 2013; Chang et al., 1997; Feng et al., 2018). It is extremely important to obtain well logging observations for establishing accurate geological models, describing the formation and flow properties of a reservoir, improving reservoir assessment, and enhancing real-time strategies for optimum well drilling, completion, and production (Ellis and Singer, 2007; Obiora et al., 2016). However, due to cost limitations or borehole problems, a specific logging curve may not have been measured in every drilled well, or be poor quality along entire well depths, or be not available at the depth intervals of interest. We aim to predict missing logging curves from available well logs based on deep learning methods.

Several researches have tried to use machine learning technology to estimate missing well logs such as acoustic logs (AC), density logs (DEN), and gamma ray (GR) from available well logs (Bukar et al., 2019;

Gowda et al., 2019, 2020; He et al., 2020; Onalo et al., 2018; Santoso et al., 2019). Chun et al. provide a reasonable approach to forecast permeability and porosity logging curves from existing well logs by constructing a back propagation neural network (BPNN) model (Fung and WongEren, 1997). For enhancing the prediction performance, the genetic algorithm was introduced to optimize the hyperparameters of artificial neural networks (ANNs) for well logging reconstruction (Mo et al., 2015). Rolon et al. produced synthetic well logs by using general regression neural network (GRNN) and achieved a better performance by comparing the proposed method with multiple regression (Rolon et al., 2009). It has been proved that the task of the logging prediction is particularly suitable for ANNs. However, conventional ANNs have several known shortcomings in the training process, such as bad local minima, poor generalization performance, and slow convergence speed, which limits the prediction performance of well logs (Gharbi and Mansoori, 2005).

To address these problems of ANNs, a deep belief network (DBN)

* Corresponding author.

E-mail address: liqun.shan.liu@gmail.com (L. Shan).

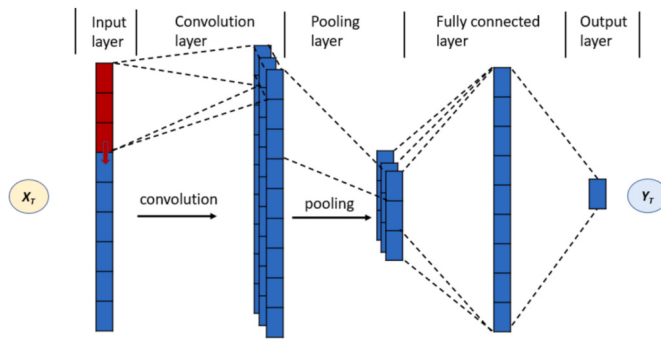


Fig. 1. Typical 1-D CNN architecture.

method was introduced to realize the porosity log prediction (Duan et al., 2018). DBN has unique advantages in initializing the weight matrix of the network and can greatly shorten the training time. Akinikawe et al. found that random forest (RF) is superior to ANN (Akinikawe et al., 2018). They used ANN, support vector machine (SVR), random forest (RF), decision trees (DT), and gradient boosting (GB) to generate conventional logging data from existing well logs. In addition, they also predicted unconventional logging curves including unconfined compressive strength (UCS) logs and photoelectric (PE) logs because the USC logs need conduct expensive core experiments and the PE logs are usually not measured during a drilling process. After comparing these algorithms, they concluded that RF is superior to other algorithms. These traditional machine learning methods are effective in forecasting missing well logging curves, but they need take much time to conduct feature engineering for achieving a good prediction performance.

In terms of the advantages of deep learning (DL) in feature extraction, numerous researchers have utilized DL algorithms, such as multi-layer perceptron neural network (MLP), convolutional neural network (CNN), long short-term memory (LSTM) and bidirectional LSTM (BiLSTM), to produce synthetize well logs (Li et al., 2019; Kim et al., 2020). Ouaadfeul and Aliouane carried out MLP to predict lithofacies from well logs data (Ouaadfeul and Aliouane, 2015). Kanfar et al. designed an inception-based temporal convolutional model to forecast the well logs during drilling (Kanfar et al., 2020a). Their method aimed to acquire both high and low frequency information of the drilling data. The predictions based on their method not only capture geological trends, but also are physically identical in geological characteristics and acoustic logs. DL networks mentioned before were developed to forecast well logging curves can effectively deal with redundant components of well logs. However, the CNN can only generate a point-to-point mapping from input logging measurements to output logging measurements. Rock properties usually show a tendency to change with depths, which is very important for geological research.

Recurrent neural network (RNN) considers the internal input from the previous step and external inputs, so the trend of change over time can be captured using the RNN technique. Zhang et al. considered well logs as a sequence of data and designed a long short-term memory (LSTM) model (LSTM is a kind of RNN) to predict whole well logging curves or missing well logs (Zhang et al., 2018); however, the model does not gauge the local shaping information of well logs. Pham et al. used a bidirectional LSTM (BiLSTM) integrated with fully connected neural networks to produce accurate predictions of AC logs from neutron porosity, GR logs, and DEN logs (Pham et al., 2020). Their proposed method improves the prediction performance by combining the local shape of well logs related to different geologic sections.

In this study, we aim to extract the spatio-temporal correlations from existing logs to forecast the target well logs. We develop a novel architecture, which couples CNN and BiLSTM with attention mechanism, for well logging prediction. This new architecture is a structure of two branches. One branch uses CNN to capture the spatial properties of well logs, and the other one conducts the feature selections by utilizing two-

layer BiLSTM with attention mechanism. Because BiLSTM can grab two-direction contextual dependencies, BiLSTM can capture the contextual information of the well logs along the depth; however, it is not capable to extract the most desired information from the captured contextual information. Extracting the most ideal features can improve the forecast accuracy. Attention mechanism is introduced to set attention weight matrix for acquiring the most desired features from the grabbed contextual information. Moreover, traditional machine learning models, CNN, BiLSTM, and other deep learning benchmark models were developed to compare with the presented models.

2. Methodology

2.1. Convolutional neural network (CNN)

CNN is a well-known deep neural network proposed by LeCun (LeCun et al., 1989). One-dimensional (1-D) CNN is used in our study because convolution kernels scan only along depth direction of the logging curves (Cheng et al., 2020). Fig. 1 illustrates the architecture of a typical 1-D CNN. The CNN is composed of a convolutional layer, pooling layer, and fully connected layer (Zang et al., 2020; Liu and Guo, 2019). The CNN captures implicit features from input data by performing convolution operations and pooling operations. Then, the extracted features are merged and fed into a fully connected layer. Finally, some an activation function is utilized to introduce nonlinearity into the output of a neuron.

The convolution layer is an essential part of the CNN (Li et al., 2016). Each convolutional layer owns multiple convolutional kernels, which are convolved with input information for capturing hidden features and forming feature maps. The feature maps go through a non-linear activation function to generate the output of the convolutional layer. The convolutional layer can be expressed as follows:

$$c_i = f(w_i * x_i + b_i) \quad (1)$$

where x_i denotes the input of convolution layer. c_i is the i^{th} output feature map, w_i is a weight matrix, $*$ represents the dot product, b_i is the bias vector, and $f(\cdot)$ represents the activation function. The rectified linear unit (ReLU) function is widely chosen as the activation function of CNNs. Mathematically, ReLU is defined as:

$$c_i = f(h_i) = \max(0, h_i) \quad (2)$$

where h_i is the element of feature maps obtained from convolutional operations.

The function of the pooling operation is to cut down the dimensions of feature maps and prevent overfitting. Max pooling is one of the most used pooling methods. This is realized by calculating the maximum value of an assigned area in feature maps according to Eqs. (3) and (4).

$$\gamma(c_i, c_{i-1}) = \max(c_i, c_{i-1}) \quad (3)$$

$$p_i = \gamma(c_i, c_{i-1}) + \beta_i \quad (4)$$

where $\gamma(\cdot)$ is the max pooling subsampling function. β_i is the bias. p_i denotes the output of maxpooling layer. Finally, the feature maps obtained through convolutional and pooling operations are fed to the fully connected layer, and then the layer calculates the final output vector, as shown below:

$$y_i = f(t_i p_i + \delta_i) \quad (5)$$

where y_i represents the final output vector, δ_i is the bias, and t_i is a weight matrix.

2.2. Bidirectional LSTM network

Conventional LSTMs are only able to make use of previous context

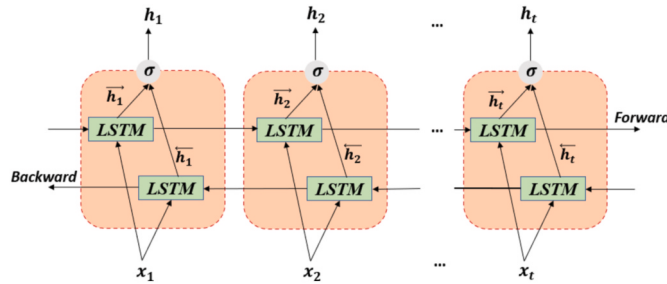


Fig. 2. Architecture of the BiLSTM.

(Hochreiter and Schmidhuber, 1997; Schuster and Paliwal, 1997). In order to access long-range information, Graves and Schmidhuber (2005) proposed the bidirectional LSTM (BiLSTM) to better grab two-direction contextual dependencies (Graves and Schmidhuber, 2005). Bidirectional architecture could extract the contextual information from both directions at the same time with forward hidden layers and backward hidden layers. The BiLSTM architecture is shown in Fig. 2.

In Fig. 2, \vec{h}_t and \overleftarrow{h}_t are the outputs of forward and backward hidden layers, respectively. The outputs of the forward layer and hidden sequences are iteratively computed using inputs in an orderly sequence from step 1 to step t , while the backward layer output and hidden sequences, are iterated from step t to 1. The outputs of the forward layer and the backward layer, \vec{h}_t and \overleftarrow{h}_t , are calculated by the standard LSTM. The BiLSTM layer yields an output vector, Y , in which each element is computed according to Eq. (6).

$$y_t = \sigma(\vec{h}_t, \overleftarrow{h}_t) \quad (6)$$

where σ function is utilized to couple the two \vec{h}_t and \overleftarrow{h}_t sequences. The σ function may be a summation function, a multiplication function, a concatenating function or an average function. The final output of a BiLSTM layer can be expressed as a vector, $Y = [y_1, y_2, \dots, y_t]$, where the last element, y_t , is the forecasted well logging value for the next depth when the BiLSTM is used to perform well log prediction.

2.3. Attention mechanism

Recently, the attention mechanism based neural networks have demonstrated success in a wide range of tasks (Povey et al., 2018; Vaswani et al., 2017; Shen et al., 2017). In a BiLSTM network with attention mechanism, the attention method takes advantage of the last cell state of the BiLSTM, or to make an alignment with the cell state of the input at the current step using the implicit state of the BiLSTM. Then, the correlation between the output state and these candidate intermediate states is computed. During the learning process, the related information can be highlighted, and the irrelevant information can be suppressed to enhance the accuracy and efficiency of prediction. The output A of the attention layer in the attentive BiLSTM network is formed according to the following Eqs. (7)–(9):

$$M = \tanh(Y) \quad (7)$$

$$\alpha = \text{softmax}(w_a^T M) \quad (8)$$

$$A = Y\alpha^T \quad (9)$$

where Y is a matrix and represents the captured features by the BiLSTM model, such as the above-mentioned matrix $Y = [y_1, y_2, \dots, y_t]$. α is a vector and represents the attention weights to features Y . w_a is the weight coefficient matrix of the attention layer. T denotes a transpose operation.

3. The proposed CNN-BiLSTM-AT hybrid model and evaluation metrics

In this section, the model architecture used in this study is described and four metrics are selected to evaluate the proposed model.

3.1. The architecture of CNN-BiLSTM-AT model

By considering the values of the well logs along depth as orderly sequences, the BiLSTM becomes an ideal method to construct synthetic well logging curves, because it is capable to not only capture information from a sequence of data but also propagate information from

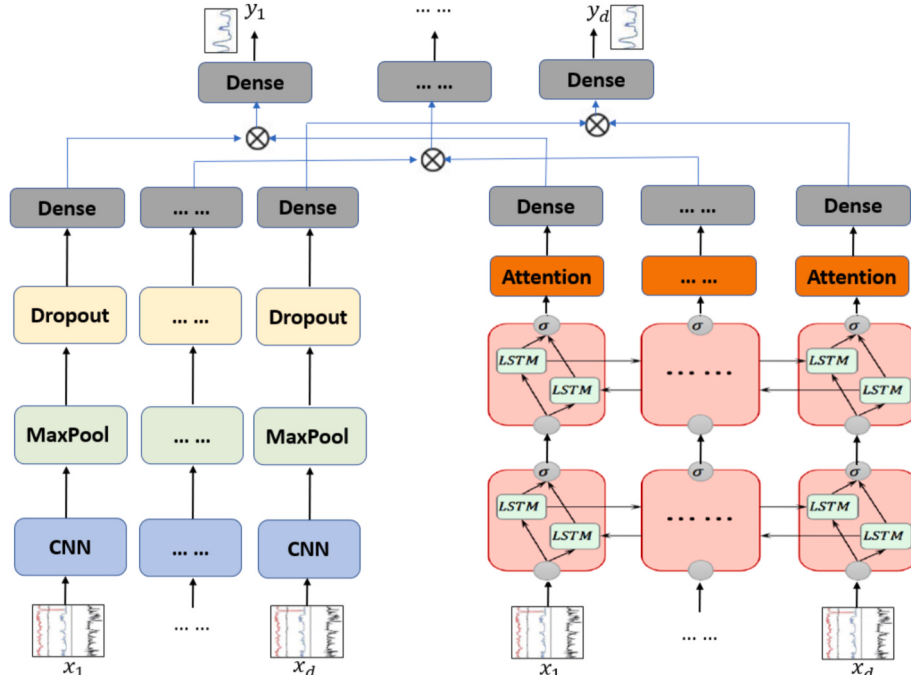


Fig. 3. Architecture of the proposed CNN-BiLSTM-AT.

Table 1

Characteristics of well logs from the dataset.

| | DEPTH | CAL | CN | CNL | DEN | GR | M2R1 | M2R3 | M2R6 | M2R9 |
|------|----------|--------|--------|--------|--------|---------|--------|--------|--------|---------|
| Mean | 1300.288 | 22.402 | 36.165 | 39.862 | 2.224 | 90.402 | 3.273 | 3.425 | 3.477 | 3.513 |
| Std | 298.499 | 0.500 | 5.647 | 7.010 | 0.091 | 12.298 | 1.859 | 1.917 | 1.963 | 1.992 |
| Min | 783.375 | 21.303 | 16.368 | 18.195 | 1.961 | 55.203 | 1.527 | 1.559 | 1.575 | 1.602 |
| 5% | 835.063 | 21.65 | 27.950 | 30.37 | 2.046 | 67.888 | 1.823 | 1.936 | 1.955 | 1.973 |
| 25% | 1041.813 | 22.046 | 32.09 | 34.917 | 2.176 | 83.509 | 2.173 | 2.305 | 2.329 | 2.353 |
| 50% | 1300.25 | 22.385 | 35.472 | 38.708 | 2.238 | 91.384 | 2.534 | 2.703 | 2.742 | 2.769 |
| 75% | 1558.813 | 22.684 | 39.766 | 43.876 | 2.286 | 98.36 | 3.534 | 3.756 | 3.823 | 3.855 |
| 95% | 1765.563 | 23.231 | 46.356 | 52.813 | 2.353 | 109.518 | 7.584 | 7.605 | 7.710 | 7.818 |
| Max | 1817.25 | 25.976 | 63.341 | 94.224 | 2.43 | 166.467 | 15.381 | 16.008 | 16.573 | 17.068 |
| | ML1 | ML2 | RA04 | RA25 | RA45 | RMSL | RT | RXO | SP | AC |
| Mean | 2.423 | 2.898 | 3.877 | 4.316 | 3.739 | 4.032 | 3.572 | 3.372 | 65.749 | 396.914 |
| Std | 0.778 | 1.166 | 2.329 | 2.627 | 1.944 | 2.390 | 2.056 | 1.907 | 9.557 | 41.261 |
| Min | 1.517 | 1.585 | 1.795 | 1.960 | 1.830 | 2.137 | 1.608 | 1.543 | 43.250 | 266.685 |
| 5% | 1.752 | 1.869 | 2.119 | 2.440 | 2.137 | 2.486 | 1.990 | 1.899 | 49.490 | 334.831 |
| 25% | 1.977 | 2.163 | 2.488 | 2.833 | 2.513 | 2.774 | 2.378 | 2.258 | 60.049 | 366.640 |
| 50% | 2.187 | 2.453 | 2.909 | 3.407 | 2.918 | 3.124 | 2.804 | 2.643 | 64.550 | 395.536 |
| 75% | 2.554 | 3.204 | 4.199 | 4.672 | 4.155 | 4.239 | 3.923 | 3.681 | 72.593 | 424.391 |
| 95% | 4.026 | 5.362 | 9.152 | 9.406 | 8.253 | 8.523 | 8.033 | 7.621 | 83.748 | 466.895 |
| Max | 11.311 | 13.29 | 16.049 | 23.868 | 13.636 | 104.588 | 17.82 | 15.905 | 89.041 | 547.203 |

adjacent depths with depth-term dependences. Meanwhile, the advantages of CNN and attention mechanism in extracting the abstract features are introduced. The architecture of the proposed CNN-BiLSTM-AT approach is illustrated in Fig. 3. This architecture is a structure of two branches, in which one branch use CNN to capture the properties of well logs and the other one implements the feature selections by utilizing a two-layer BiLSTM with the attention mechanism. The features from two branches are concatenated and fed into the last dense layer to generate the target predictions.

For well logging measurements, the defined sequence matrix X along depth can be expressed by Eq. (10).

$$X = \begin{bmatrix} x_1^1 & x_1^2 & \dots & x_1^n \\ x_2^1 & x_2^2 & \dots & x_2^n \\ \vdots & \vdots & \ddots & \vdots \\ x_i^1 & x_i^2 & \dots & x_i^n \\ \vdots & \vdots & \ddots & \vdots \\ x_d^1 & x_d^2 & \dots & x_d^n \end{bmatrix} \quad (10)$$

where the set $x_d = (x_d^1, x_d^2, \dots, x_d^n)$ is the attribute values of n well logs at the depth d . The set $x^n = (x_1^n, x_2^n, \dots, x_i^n, \dots, x_d^n)$ is the values of a certain well logging curve along the depth, such as GR, CNL, SP, etc. $Y = (y_1, y_2, \dots, y_i, \dots, y_d)$ is the measurements of forecasted well logs. The X and Y is the inputs and outputs of the CNN-BiLSTM-AT model, respectively.

In the CNN branch, the X is fed to convolutional operators. 1-D convolutional operators slide 128 filters with the same window size of 1 over depth sequences to capture the low-level implicit features from the raw well logs. Then, a max-pooling operation is conducted to reduce the dimension of feature maps. A dropout operation is utilized to prevent the overfitting of the CNN. ReLU is used as the nonlinear activation function of this layer. Finally, a flatten layer is used to change the dimension direction and a dense layer with 100 neurons is used to carry out a linear operation.

In the BiLSTM-AT branch, the two-layer BiLSTM captures the contextual information from original well logs. Each BiLSTM with 50 cell units not only learn the knowledge from the preceding term of current logging point but also obtain the knowledge from succeeding term of current log sequence, so the features grabbed by BiLSTM can be thought of as two different representations of the well logs. In the BiLSTM layer, the tanh function is selected as the nonlinear activation function. In the attention layer, attention mechanism can highlight the key features of the logging curves to reduce the influences of non-key features in well logs. The attention layer consists of a fully connected

unit with 100 neurons and a *softmax* activation function. The features extracted from the BiLSTM are fed to the attention layer, then are added to the output of the fully connected unit. The attention layer is followed by one dense unit. The output of the attention layer is passed into the dense unit with 100 neurons.

The outputs from the CNN branch and the BiLSTM-AT branch are combined before being fed into the last dense layer with 1 neuron. The activation function of the dense layer is *tanh*. Finally, the predicted Y is yielded from the CNN-BiLSTM-AT model.

3.2. Evaluation metrics

In our experiments, four predictive metrics are calculated to assess the performance of the prediction results of well logs, namely root mean square error (RMSE), mean absolute percentage error (MAPE), mean absolute error (MAE), and person correlation coefficient (PCC) (Biber et al., 1998). These evaluation metrics indicate the deviation of prediction of proposed models. They are defined as

$$\text{RMSE} = \sqrt{\frac{1}{n} \sum_{d=1}^m [y_{od} - y_{pd}]^2} \quad (11)$$

$$\text{MAE} = \frac{1}{m} \sum_{d=1}^m \left| \frac{y_{od} - y_{pd}}{y_{od}} \right| \quad (12)$$

$$\text{MAPE} = 100 \times \frac{1}{m} \sum_{d=1}^m \frac{|y_{od} - y_{pd}|}{y_{od}} \quad (13)$$

$$PCC = \frac{\sum_{d=1}^m (y_{od} - \bar{y}_o)(y_{pd} - \bar{y}_p)}{\sqrt{\sum_{d=1}^m (y_{od} - \bar{y}_o)^2} \sqrt{\sum_{d=1}^m (y_{pd} - \bar{y}_p)^2}} \quad (14)$$

where m is the number of points in well logging curves, y_o is the measured data, \bar{y}_o is the mean of y_o , y_p is the predicted data, and \bar{y}_p the mean of y_p . The RMSE denotes the standard deviation between the predictions of the model and actual logs. The MAE can describe an average difference between the predictions and the actual measurements. The MAPE expresses accuracy as a percentage. PCC can describe the linear dependence between the forecasted and real measurements of well logs. Among these metrics, smaller RMSE, MAPE, and MAE indicate that the model has better performance, while larger PCC values indicate that the model has better performance.

The objective of the well log prediction based on the CNN-BiLSTM-AT hybrid network is to minimize the error between the real and

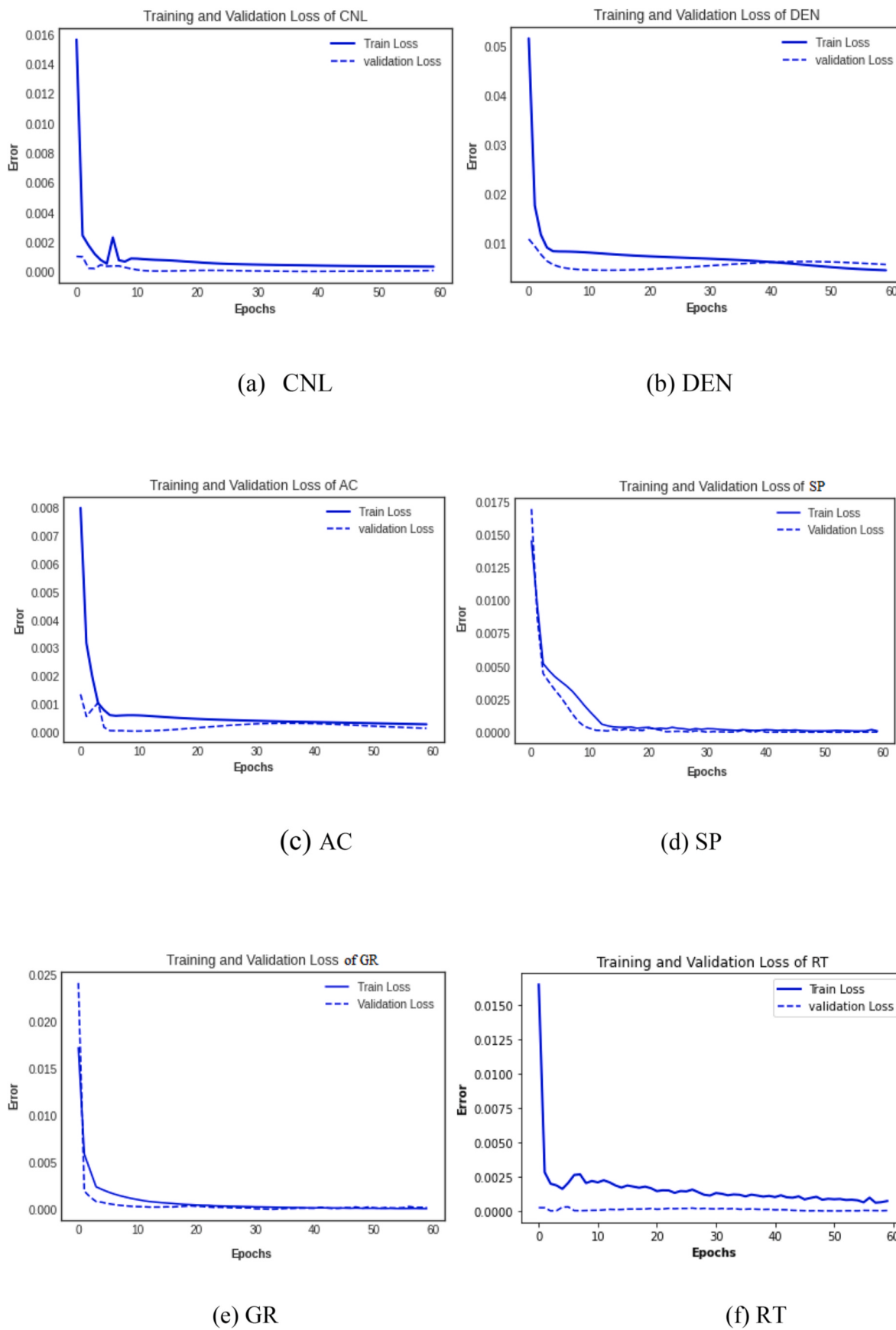


Fig. 4. Convergence of the errors on the training and validation dataset.

Table 2

Average prediction errors and standard deviations on testing data.

| Models | RMSE | MAE | MAPE |
|---------------|----------------|---------------|---------------|
| Model for CNL | 2.3140±0.0485 | 1.6553±0.0382 | 4.7606±0.1473 |
| Model for GR | 4.0614±0.0380 | 3.0989±0.0477 | 3.4654±0.0749 |
| Model for AC | 10.3855±0.2017 | 7.8516±0.1822 | 2.2481±0.0598 |
| Model for SP | 2.8519±0.0890 | 2.3836±0.0698 | 2.9900±0.0871 |
| Model for DEN | 0.0110±0.0027 | 0.0087±0.0032 | 0.3834±0.1427 |
| Model for RT | 0.0683±0.0146 | 0.1771±0.0091 | 6.1559±0.0613 |

predicted logs at every depth. During the whole learning process, RMSE is set as the objective function of the CNN-BiLSTM-AT network.

4. Experiments and results

To evaluate the performance of the proposed approach, a dataset including 152,969 samples were collected from a highly heterogenous reservoir at the Gangdong oilfield in China. The method is examined on the prediction of compensated neutron logs (CNL), acoustic (AC), spontaneous potential (SP), gamma-ray (GR), density (DEN), and formation resistivity (RT) from other nineteen log properties, respectively.

All experimental studies were carried out in the Python 3.8 compiling environment using a deep learning workstation with RTX 2080 Ti. All artificial intelligence models were developed using the TensorFlow (Abadi et al., 2016).

4.1. Study area

For evaluating the well log prediction by the proposed method in this study, well logs were collected from the Gangdong Oilfield in China. The study area is mainly concentrated in the vicinity of the Beidagang second-class fault structural zone in the middle of the Huanghua formation. The target layer of the work area is mainly composed of the Minghuazhen formation and Guantao formation of the Upper Tertiary. Minghuazhen has created a meandering riverbed. The channel sand bodies are distributed in strips on the plane, and the thickness of a single sand layer is generally 3–16 m. The Guantao formation is a braided river deposit, with single-layer river channels distributed in contiguous areas. The channel sand bodies have a large width and a thickness of 6–20 m. The first member of the east is a delta deposit, and the sand bodies develop in a northwest-south east direction. The fluvial facies single sand body and its internal architectural structure are very complicated.

The lithology in the Minghuazhen formation consists of green gray, gray-green medium sandstone, siltstone, fine sandstone, brown-red mudstone, argillaceous siltstone, and silty mudstone. The electrical measurements along depths are bell-shaped and toothed bell-shaped. It demonstrates a characteristic of positive cycles. The lithology in the Guantao formation is mainly composed of gray-white sandstone, gray siltstone, yellow-brown conglomerate sandstone, fine sandstone, medium sandstone, coarse sandstone, gray-green and purple-red mudstone. The vertical channel is superimposed over multiple periods to generate a thick sand layer with relatively coarse grain size. More sand and less mud exist on the profile, so the electrical signals appear as a combination of low amplitude gear-shaped and gear-box-shaped curves. In non-main channel deposition areas, the sand layer is relatively thin, mudstone is added to thicken, so the curves seem like a combination of box-bell-shaped curves and box-shaped.

Analyzing the rock core of the study area shows that the porosity is essentially between 20% and 40%, and the average porosity of the reservoir physical property is 31.18%. The permeability of the reservoir physical property is mainly between 20mD and 6575mD. The permeability variation coefficient was approximated to be 0.9, that indicates that the reservoir characteristics and physical properties of the study area are dominated by the strong rock mechanical heterogeneity.

4.2. Dataset

A total of 37 wells from the study area comprise the dataset for this study. Each well in the dataset has twenty logging attributes, including acoustic (AC), spontaneous potential (SP), caliper (CAL), neutron (CN), density (DEN), flushed zone resistivity (RXO), natural gamma ray (GR), formation resistivity (RT), compensated neutron log (CNL), high resolution induction logging (M2R1, M2R3, M2R6, and M2R9), microlog 1 (ML1), microlog 2 (ML2), 0.4m potential (RA04), 2.5m potential (RA25), 4.5m potential (RA45), microspherical focused resistivity (RMSL), and depth (DEPTH). That means that, based on the proposed method, a whole set of well logging curves can be synthetically generated for these 37 wells.

It is significant to carry out data preprocessing for improving the accuracy of data prediction, including data cleaning, standardization and normalization.

Data cleaning: Data cleaning aims to improve data quality of well logs. Five wells in the research area are firstly selected by professional engineers, and then the outliers and noise information are discarded by a mean substitution method and the scatter plot visualization (Barducci et al., 2007).

Standardization: Data standardization is used to reduce the systematic errors of well logs observed by different measuring equipment at different times. It can keep all the well logs conform with the same standard. Meanwhile, data standardization has the impact of speeding up training process and preventing gradient explosion of neural networks (Hrynaszkiewicz, 2010).

Normalization: Data normalization is essential to ensure that the models will be successfully trained, because it can generate high-quality data that can be input to any learning algorithm. The logging data have a wide range of values, so they need to be scaled to the same range of values to speed up the learning process. In our experiments, the input sequences were scaled to the range of 0–1 because a sigmoid function is used as the activation functions of the gating units in the BiLSTM. Discrete well log data are normalized to [0,1] according to Eq. (15).

$$x_i = \frac{(x_o - \bar{x})}{(x_{max} - x_{min})} \quad (15)$$

where x_i are the normalized values of a well log curve at depth d , x_{min} refers to the minimum value, x_{max} denotes the maximum value.

After the data preprocessing, the dataset with the total samples 152,969 is formed in the case study. The characteristics of well log samples is shown in Table 1. 8792 samples of well logs in well Gang-11-11 are reserved to verify our proposed method. We used the rest of the remaining samples 90% as training set. The models for predicting kinds of well logs were trained and the hyperparameters of the models were determined by using a 10-fold cross-validation approach (Arlot and Celisse, 2010). In the training stage, based on the 10-fold cross-validation approach, the data from the training set was divided into ten parts, and the tenth set was taken as the validation set to test the model. The remaining nine sections were taken as the training set to train the model. In the evaluation stage, 8792 samples from Gang-11-11 were fed into the trained model, and the predictions would be obtained.

4.3. Experiment results

In our experiments, six models were trained and used for forecasting well logs including CNL, DEN, AC, SP, GR, and RT. The convergence rate during the optimization of the hyperparameters for each model, expressed as the RMSE error on the training and validation dataset, is depicted in Fig. 4. As shown in Fig. 4, the loss functions of the proposed models for the oilfield case can quickly decrease and become stable which means the models are well trained and can be used to predict the missing well logs.

The averaged prediction results and the standard deviations of 30

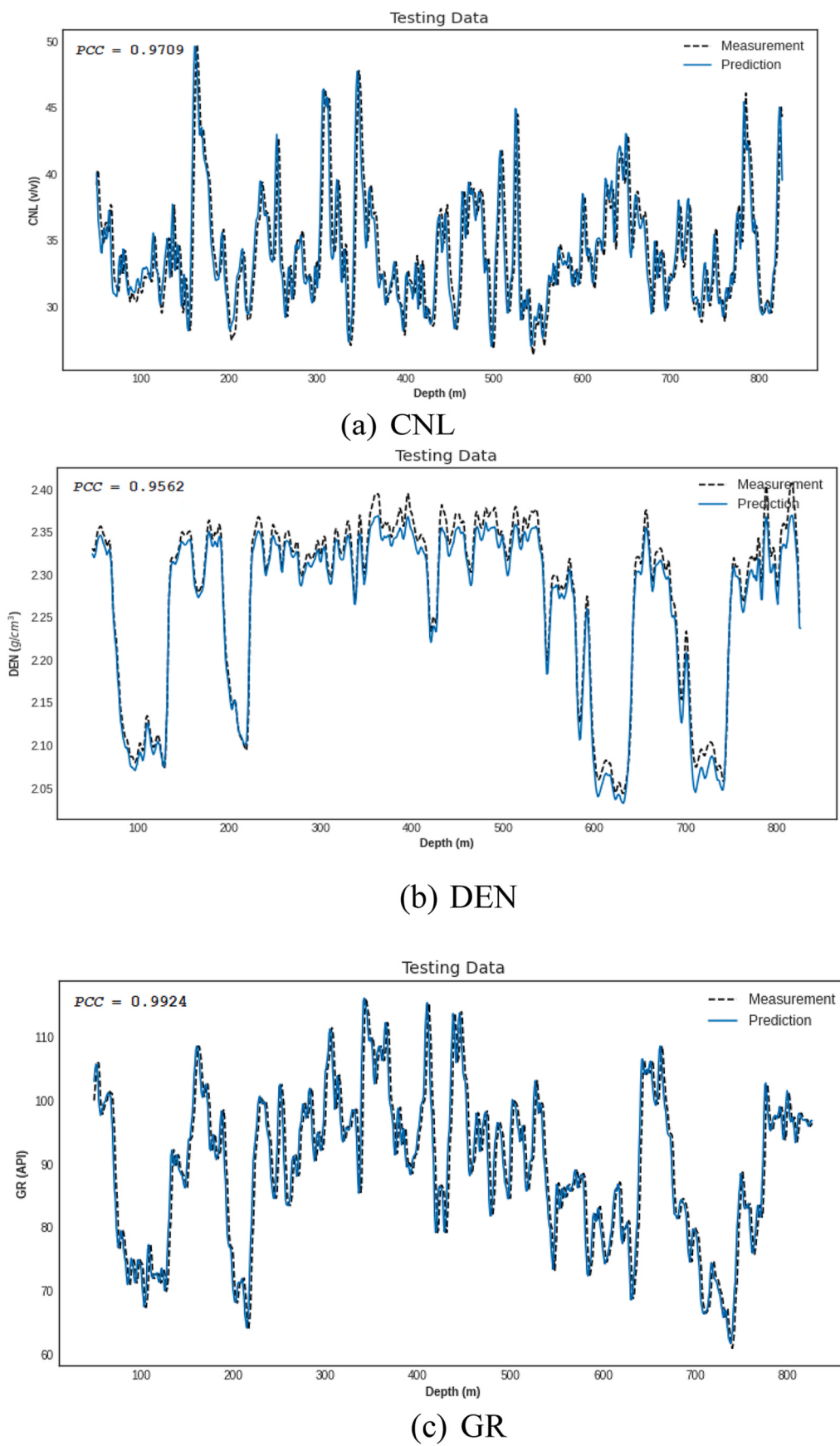


Fig. 5. Measurements vs. predictions using CNN-BiLSTM-AT.

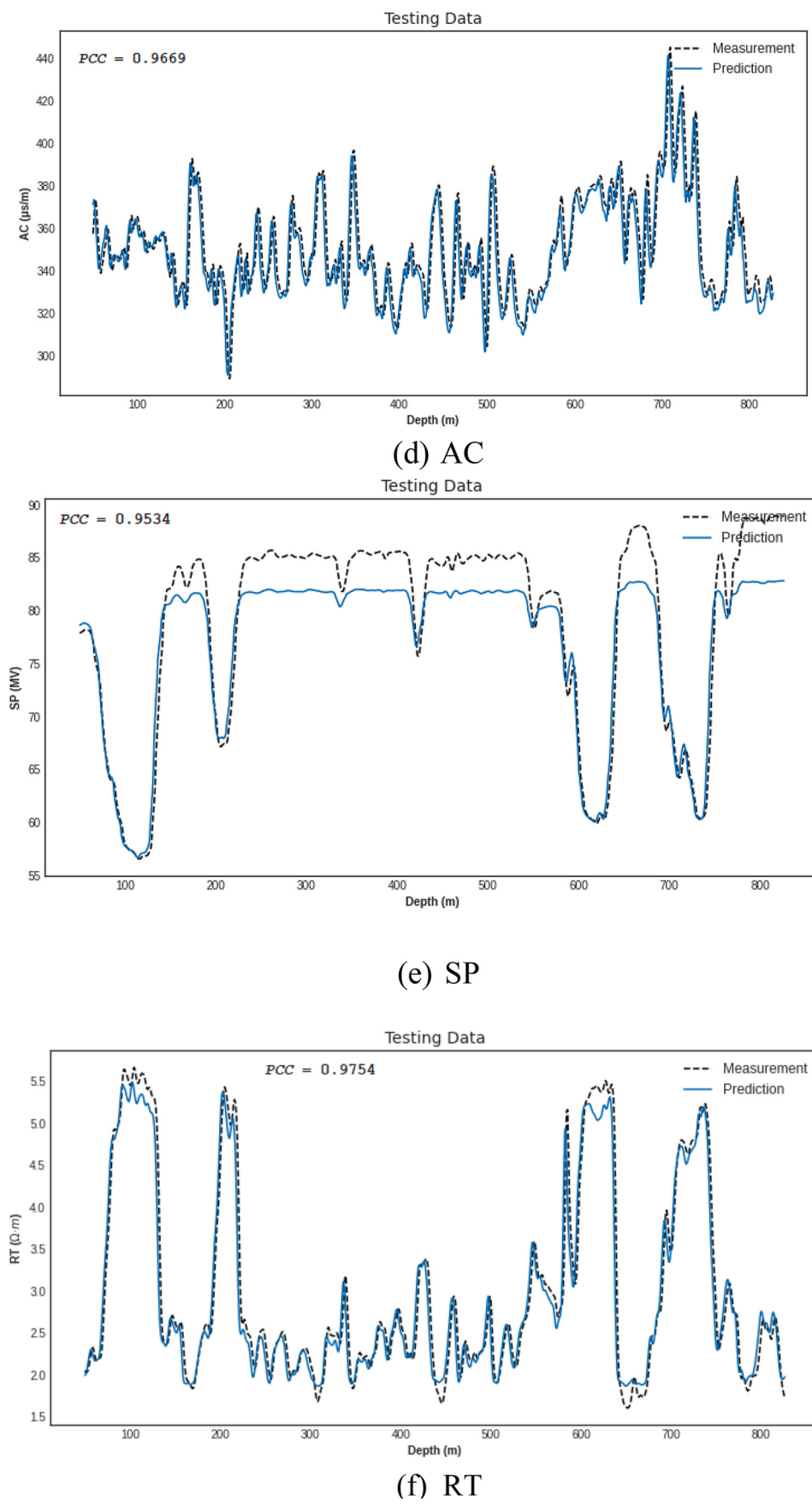


Fig. 5. (continued).

Table 3

Comparison of CNN-BiLSTM-AT model with classical machine learning models for predicting CNL well logs.

2) Comparison with models based on deep learning

| Models | RMSE | MAE | MAPE |
|---------------|----------------------|----------------------|----------------------|
| DT | 8.1663±0.1901 | 5.2052±0.0533 | 9.6921±0.1485 |
| SVR | 7.9725±0.0623 | 4.7361±0.0882 | 9.3777±0.0437 |
| RF | 6.0063±0.1912 | 3.6439±0.1056 | 8.0978±0.0291 |
| MLP | 6.9704±0.1580 | 3.7460±0.0979 | 8.1036±0.0887 |
| CNN-BiLSTM-AT | 2.3140±0.0485 | 1.6553±0.0382 | 4.7606±0.1473 |

independent experiments of each model under each setting are reported in [Table 2](#). The CNN-LSTM-AT model for predicting CNL well logs achieves the best RMSE, 2.3140, MAE, 1.6553, and MAPE, 4.7606. To forecast GR logging curves, the CNN-LSTM-AT model is trained to obtain the best RMSE, 4.0614, MAE, 3.0989, and MAPE, 3.4654. When generating the best synthetic AC well logs, we obtained the RMSE, 10.3885, MAE, 7.8516, and MAPE, 2.2481. The CNN-LSTM-AT model for predicting SP logs achieves the best RMSE, 2.8519, MAE, 2.3836, and MAPE, 2.9900. To forecast DEN logging curves, the CNN-LSTM-AT model is trained to achieve the best RMSE, 0.0110, MAE, 0.0087, and MAPE, 0.3834. When generating the best synthetic RT well logs, we acquired the RMSE, 0.0683, MAE, 0.1771, and MAPE, 6.1559.

[Fig. 5](#) shows the measurements and predictions of CNL, DEN, AC, SP, GR, and RT well logs on testing dataset using the proposed CNN-BiLSTM-AT method. We can see from these figures that, for forecasting CNL, DEN, AC, GR, and RT logs, the proposed method can achieve a good fitting between the predicted and actual measurements, and the PCC is greater than 0.9534. From [Fig. 5\(e\)](#), it can be seen when we produced synthetic SP well logs by using the CNN-BiLSTM-AT method, the PCC is 0.9534. The prediction curve could not completely capture the trends of the measured data. That is because the study area is highly heterogeneous reservoirs representing a complex geological condition, it is difficult to acquire the predictions to be completely consistent with real measurements. However, for geological applications, valuable information is stored in the changing trend of the well logging curves, and the single measurement at each depth has little effect on the practical engineering field. By comparing the measured values and predicted values, the CNN-LSTM-AT can accurately predict the trend of well logs that is indispensable for meeting petroleum engineering demand. These well log predictions are useful for establishing more accurate geological models, improving reservoir evaluation accuracy, and optimizing well drilling and completion strategies.

4.4. Comparison with baseline models

In this section, we compared the results of the well log predictions using the proposed CNN-BiLSTM-AT method with those using traditional machine learning methods and artificial intelligence models based on deep learning.

1) Comparison with traditional machine learning methods

Table 4

Comparison of CNN-BiLSTM-AT model with DL-based models for predicting CNL well logs.

| Model | Number of layers | | | | | | | |
|---------------|------------------|---------------|---------------|---------------|--------|--------|--------|--------|
| | N = 1 | | N = 2 | | N = 3 | | N = 4 | |
| | MAE | MAPE | MAE | MAPE | MAE | MAPE | MAE | MAPE |
| RNN | 1.9421 | 5.8554 | 2.0127 | 6.1105 | 2.0989 | 6.4484 | 2.3773 | 7.3708 |
| CNN | 1.7097 | 4.9150 | 1.8831 | 5.6449 | 1.8472 | 5.4715 | 2.3594 | 7.4427 |
| LSTM | 1.7900 | 5.3032 | 1.7688 | 5.2002 | 1.9928 | 6.0474 | 2.2482 | 7.0075 |
| BiLSTM | 1.7493 | 5.1356 | 1.7762 | 5.2179 | 1.8788 | 5.6173 | 2.0122 | 6.1144 |
| BiLSTM-AT | 1.7490 | 5.1321 | 1.7606 | 5.1755 | 1.7826 | 5.2438 | 1.9782 | 6.4138 |
| CNN-BiLSTM-AT | 1.6857 | 4.8332 | 1.6553 | 4.7606 | 1.6919 | 4.8733 | 1.6910 | 4.8649 |

As mentioned in the introduction, many classical machine learning baseline models used in well log forecasting problems, like DT, SVR, RF, and ANN. Among these approaches, the MLP has become a popular method for forecasting the well logs, and tree based and SVR are very efficient techniques for the well log prediction. These classical algorithms were carried out to generate synthetic well logs in our experiments. When developing the SVR model, the radial basis function (RBF) is chosen as a kernel function. When building the RF model, 150 trees are developed, and there is no limitation in the maximum depth of the trees. For the MLP method, the MLP model consists of two hidden layers with 500 nodes in each layer. The hyperparameters of these models are optimized through a grid search method and 10-fold cross-validation method.

Taking the predictions of CNL logs as an example, we carried out 30 independent experiments of each model under each setting. [Table 3](#) demonstrates three evaluation metrics, RMSE, MAE, and MAPE, obtained from the DT, SVR, RF, MLP and CNN-BiLSTM-AT algorithms for the CNL predictions. The number of input time lags in this experiment is set to 1. Among the classic machine learning algorithms, RF works much better, with the mean MAE of 3.6439, than the SVR method and DT method, which is due to the majority voting mechanism of the RF method. The MLP whose mean MAE is 3.7460 performs very close to the RF model. Our proposed CNN-BiLSTM-AT achieves the mean MSE of 1.6553 that obviously outperform those obtained by using the MLP and RF approaches. The hybrid structure of CNN, BiLSTM and attention mechanism may be the reasons. From the comparison among these algorithms, the proposed CNN-BiLSTM-AT model is clearly superior to the traditional machine learning models developed in this experiment.

The CNN-BiLSTM-AT as a type of deep learning algorithms is proposed aiming at predicting the well logs, and thus, other deep learning models with the ability of predicting well logging curves are developed for the comparison with the proposed model in this section. The standard deep BiLSTM and CNN are compared because the proposed model makes up of the BiLSTM and CNN. LSTM and standard RNN adding a fully connected deep neural network layer are also investigated. To measure the influence of attention mechanism to the well log prediction, a multilayer BiLSTM model combining attention mechanism (BiLSTM-AT) is also developed in this experiment.

Consider the influence of hidden neuron nodes and the depth of the neural networks, namely the hyperparameters of the models, all the models implemented in this section carried out the genetic algorithm to optimize these hyperparameters. [Table 4](#) shows the comparison results of the average of 30 runs of each model under each setting. The headers on horizontal direction of the table represents the number of the neural network layers of each deep learning models. Taking into account the influence of the number of layers of the neural network, each deep learning models developed in this study achieve the best performance at a specific number of layers, and their evaluation metrics have different scores with the number of layers from one to four. When the CNN-BiLSTM-AT model used to predict CNL logging curves has one CNN layer and two BiLSTM layers, it achieves the best performance.

The proposed CNN-BiLSTM-AT outperforms the other deep learning algorithms under all kind of number of layers. When the CNN-BiLSTM-

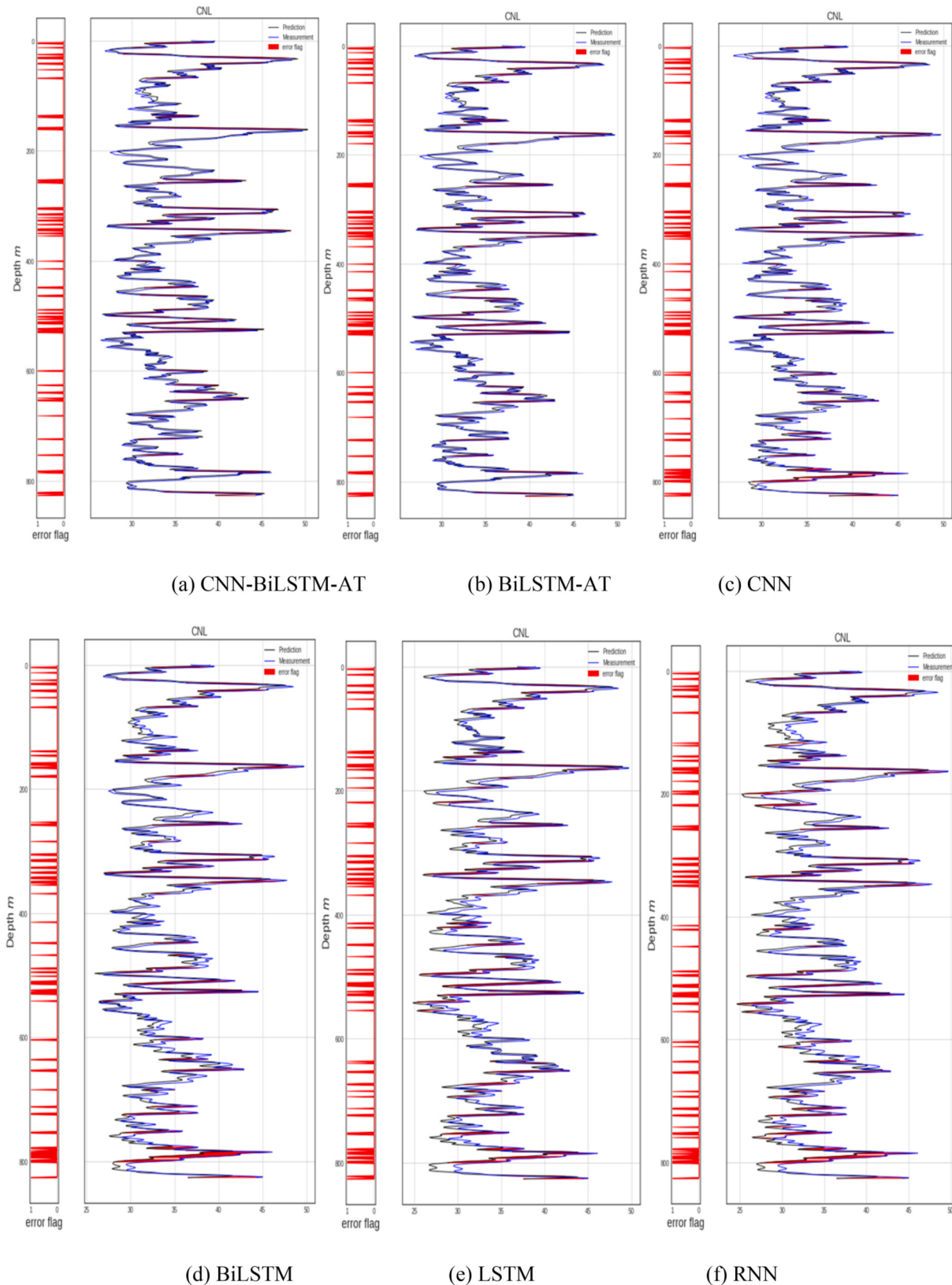


Fig. 6. Error flag of CNL well log prediction from deep learning algorithms.

AT has two layers, it yields the best mean MAE, 1.6553, and mean MAPE, 4.7606. The testing errors of multilayer RNN, CNN, LSTM, BiLSTM and BiLSTM-AT are greater than those of the CNN-BiLSTM-AT model. They yield their best mean MAEs of 1.9421, 1.7097, 1.7688,

1.7493, and 1.7490, respectively. It should be noted that, for the one-layer case, RNN, CNN, BiLSTM and BiLSTM-AT models get the best performance in our case study shown in Table 4. It indicates that one-layer neural network models can be good enough for capturing

features, but the hybrid neural network structure of the CNN-BiLSTM-AT is more satisfactory to predict the target well logs.

Fig. 6 shows the effects of RNN, CNN, LSTM, BiLSTM, BiLSTM-AT and CNN-BiLSTM-AT in the prediction of CNL logs. Compared with the measurements from the oilfield, the predictions from six deep learning models have a high fitting degree, which indicates that the deep learning method can forecast the changing tendency of target CNL curves accurately. The red error flags in Fig. 6 indicate the predictions using the RNN method has the largest error flags. The forecast accuracy of well logs obtained by the LSTM and BiLSTM methods have been enhanced. Using the combination of the BiLSTM algorithm and attention mechanism, the well log prediction accuracy has been further improved obviously. The prediction accuracy from the CNN method is no less than the result using the BiLSTM model. The proposed CNN-BiLSTM-AT method achieves the highest fitting degree. Therefore, the CNN-BiLSTM-AT can be a powerful tool for predicting such well logging sequences.

5. Discussion

Current studies in forecasting the missing well logs by using machine learning/deep learning have not considered the spatial features and temporal characteristics simultaneously, we presented a hybrid neural network based on CNN and BiLSTM with the attention mechanism in this study. The CNN focuses on capturing the spatial properties of well logs, the BiLSTM extracts the temporal features, and the attention mechanism is used to focus on strengthening the important information. The spatio-temporal correlations from CNN and BiLSTM with the attention mechanism are merged to fulfill the target well log prediction. The CNN-BiLSTM-AT method was used to implement the predictions of CNL, DEN, AC, SP, GR, and RT well logs. Through the CNN-BiLSTM-AT method, all loss functions can quickly decrease and become stable which means the models are well trained and can be used to predict. For all six logging curves, the PCC obtained is greater than 0.9534. The experimental results indicate the proposed method can achieve a good fitting degree between the predicted and actual well logs.

The method of automatically producing well logs based on the CNN-BiLSTM-AT proposed in this study can reduce the cost of oil and gas development to a certain extent. In the unconventional oil and gas development, abundance of well logs can help engineers improve their understanding of the formation, which gives rise to lower the cost in the perforation clusters during well completion (PARSHALL, 2015). The proposed deep learning method for the synthetic well logs generation can also be extended to the prediction of real-time logging curves with the help of the real-time drilling data, which can help management choose better strategies during the real-time drilling, especially for directional wells and production wells (Kanfar et al., 2020b). In addition, our trained models can be modified to use in any areas of interest by adjusting the hyperparameters. For a certain newly drilled well, any required well logging curves can be automatically synthesized based on all kinds of available well logs around the new well and the trained CNN-BiLSTM-AT network. The low cost and effectiveness of producing well logs based on the deep learning technique makes it possible to employ the deep learning method on a large scale, which is conducive to assessment and analysis at the formation and basin level.

In the future, we will carry out the investigation in the uncertainty of the predicting model. The results of an uncertainty analysis would provide the probability weighted values of the predictions, help make optimal decisions in view of imperfect knowledge, measure the risk or the dispersion of the outcome, and reveal the value of information for key variables, so the uncertainty analysis can provide the information about the model robustness and the reliability of the predicted results (Ghahramani, 2015; Feng, 2020, 2021; Feng et al., 2021). In addition, the results with a high certainty can bring with the additional confidence to practitioners in oil and gas fields.

6. Conclusions

This paper aims to address the problem of well logging curves shortages. We proposed a well log prediction method based on the integration of convolutional neural network and bidirectional long short-term memory with attention mechanism. A case study with the proposed learning model was conducted on the data from a highly heterogeneous reservoir at the Gangdong oilfield in China. The prediction performance of the models is validated. The proposed method can be extended to other oilfields because these trained models are capable to effectively generate missing well logs from any area of interest by adjusting the hyperparameters. The precise predictions of well logs enable geological engineers to better understand the formation and improve the design of drilling and completion strategies, which leads to lower costs and enhanced productivity in oil and gas development.

Credit author statement

Liqun Shan: Conceptualization, Methodology, Writing – original draft, Yanchang Liu: Investigation, Formal analysis, Validation, Min Tang: Resources, Data preprocessing, Ming Yang: Data curation, Writing- Reviewing and Editing, Xueyuan Bai: Visualization

Declaration of competing interest

The authors declare that they have no known competing financial interests or personal relationships that could have appeared to influence the work reported in this paper.

Acknowledgement

This research was supported by Northeast Petroleum University Foundation Founding No. 2018GP2D-04 and No. 2018QNQ-06. We gratefully acknowledge the helpful comments of the editor and anonymous reviewers.

References

- Abadi, M., Barham, P., Chen, J., Chen, Z., Davis, A., Dean, J., et al., 2016. TensorFlow: A System for Large-Scale Machine Learning.
- Akinnikawe, O., Lyne, S., Roberts, J., 2018. Synthetic well log generation using machine learning techniques. In: In Proceedings of the 6th Unconventional Resources Technology Conference, Houston, TX, USA, July.
- Arlot, S., Celisse, A., 2010. A survey of cross-validation procedures for model selection. *Stat. Surv.* 4, 40–79.
- Avseth, P., et al., 2013. Rock physics modelling of 4D time-shifts and time-shift derivatives using well log data-a North Sea demonstration. *Geophys. Prospect.* 61 (2), 380–390. <https://doi.org/10.1111/j.1365-2478.2012.01134.x>.
- Barducci, A., Guzzi, D., Marcoionni, P., et al., 2007. Assessing noise amplitude in remotely sensed images using bit-plane and scatterplot approaches[J]. *IEEE Trans. Geosci. Rem. Sens.* 45 (8), 2665–2675. <https://doi.org/10.1109/tgrs.2007.897421>.
- Biber, D., Conrad, S., Reppen, R., 1998. Corpus Linguistics (Investigating Language Structure and Use) || Statistical Measures of Lexical Associations, vol. 7. Cambridge University, pp. 265–268. <https://doi.org/10.1017/CBO9780511804489>.
- Bukar, I., Adamu, M.B., Hassan, U., 2019. A Machine Learning Approach to Shear Sonic Log Prediction. August 5). Society of Petroleum Engineers. <https://doi.org/10.2118/198764-MS>.
- Chang, H.-C., Chen, H.-C., Fang, J.-H., 1997. Lithology determination from well logs with fuzzy associative memory neural network. May *IEEE Trans. Geosci. Rem. Sens.* 35 (3), 773–780.
- Cheng, Hengda, Chen, Huanxin, Li, Zhengfei, Cheng, Xiangdong, 2020. Ensemble 1-D CNN diagnosis model for VRF system refrigerant charge faults under heating condition. *Energy Build.* 224, 110256.
- Duan, Youxiang, et al., 2018. Research and application on DBN for well log interpretation. *J. Appl. Sci.* 36 (4), 689–697.
- Ellis, D.V., Singer, J.M., 2007. Well Logging for Earth Scientists. Berlin/Heidelberg, second ed. Springer, Germany, ISBN 978-1-4020-3738-2.
- Feng, R., 2020. Lithofacies classification based on a hybrid system of artificial neural networks and hidden Markov models. *Geophys. J. Int.* 221 (3), 1484–1498.
- Feng, R., 2021. Improving uncertainty analysis in well log classification by machine learning with a scaling algorithm. *J. Petrol. Sci. Eng.* 196, 2021,107995.
- Feng, R., Luthi, S.M., Gisolf, D., Angerer, E., 2018. Reservoir lithology determination by hidden Markov random fields based on a Gaussian mixture model. *Nov IEEE Trans. Geosci. Rem. Sens.* 56 (11), 6663–6673.

- Feng, R., Grana, D., Balling, N., 2021. Uncertainty quantification in fault detection using convolutional neural networks. *Geophysics*. <https://doi.org/10.1190/geo2020-0424.1>.
- Fung, Chun Che, Wong, Kok Wai, Eren, H., 1997. Modular artificial neural network for prediction of petrophysical properties from well log data. *IEEE Transactions on Instrumentation and Measurement* 46 (6), 1295–1299. <https://doi.org/10.1109/IMTC.1996.507317>.
- Gahramani, Z., 2015. Probabilistic machine learning and artificial intelligence. *Nature* 521, 452–459. <https://doi.org/10.1038/nature14541>.
- Gharbi, R.B.C., Mansoori, G.A., 2005. An introduction to artificial intelligence applications in petroleum exploration and production. *J. Petrol. Sci. Eng.* 49 (3–4), 93–96.
- Gowida, A., Elkhatatny, S., Abdulraheem, A., 2019. Application of artificial neural network to predict formation bulk density while drilling. *Petrophysics* 60, 660–674.
- Gowida, A., Elkhatatny, S., Al-Afnan, S., Abdulraheem, A., 2020. New computational artificial intelligence models for generating synthetic formation bulk density logs while drilling. *Sustainability* 12, 686.
- Graves, A., Schmidhuber, J., 2005. Framewise phoneme classification with bidirectional Lstm and other neural network architectures. *Neural Network*, 18 (5–6), 602–610.
- He, X., Santos, R., Hoteit, H., 2020. Application of machine-learning to construct equivalent continuum models from high-resolution discrete-fracture models. In: Presented at International Petroleum Technology Conference, Dhahran, Saudi Arabia, 13 - 15 January. IPTC-20040-MS. <https://doi.org/10.2523/IPTC-20040-MS>.
- Hochreiter, S., Schmidhuber, J., 1997. Long short-term memory. *Neural Comput.* 9 (8), 1735–1780.
- Hrynaszkiewicz, Iain, 2010. A call for BMC Research Notes contributions promoting best practice in data standardization, sharing and publication. *BMC Res. Notes* 3 (1), 235–237. <https://doi.org/10.1186/1756-0500-3-235>.
- Kanfar, R., Shaikh, O., Yousefzadeh, M., Mukerji, T., 2020a. January 13). Real-time well log prediction from drilling data using deep learning. International Petroleum Technology Conference. <https://doi.org/10.2523/IPTC-19693-MS>.
- Kanfar, R., Shaikh, O., Yousefzadeh, M., Mukerji, T., 2020b. Real-Time Well Log Prediction from Drilling Data Using Deep Learning. In: Paper Presented at the International Petroleum Technology Conference, Dhahran, Kingdom of Saudi Arabia, January 2020. <https://doi.org/10.2523/IPTC-19693-MS>.
- Canada, Geofluids Kim, Sungil, Kim, Kwang Hyun, Min, Baehyun, Lim, Jungtek, Lee, Kyungbook, 2020. Generation of Synthetic Density Log Data Using Deep Learning Algorithm at the Golden Field in Alberta, Article ID 5387183, p. 26.
- LeCun, Y., Boser, B., Denker, J.S., Henderson, D., Howard, R.E., Hubbard, W., Jackel, L. D., 1989. Backpropagation applied to Handwritten Zip Code Recognition 1 (4), 541–551.
- Li, Y., Hao, Z., Lei, H., 2016. Survey of convolutional neural network. *J. Comput. Appl.* 9 (36), 2508–2515.
- Li, Y., Sun, R., Horne, R., 2019. Deep Learning for Well Data History Analysis. September 23). Society of Petroleum Engineers. <https://doi.org/10.2118/196011-MS>.
- Liu, Gang, Guo, Jiabao, 2019. Bidirectional LSTM with attention mechanism and convolutional layer for text classification. *Neurocomputing* 337, 325–338.
- Mo, X., Zhang, Q., Li, X., 2015. Well logging curve reconstruction based on genetic neural networks. Aug in Proc. 12th Int. Conf. Fuzzy Systems Knowl. Discovery (FSKD) 1015–1021.
- Obiora, Daniel N., et al., 2016. Reservoir characterization and formation evaluation of a “Royal onshore field”, Southern Niger Delta using geophysical well log data. *J. Geol. Soc. India* 87 (5), 591–600. <https://doi.org/10.1007/s12594-016-0433-6>.
- Onalo, David, Adedigba, Sunday, Khan, Faisal, James, Lesley A., Butt, Stephen, 2018. Data driven model for sonic well log prediction. *J. Petrol. Sci. Eng.* 170, 1022–1037.
- Ouadfeul, S.A., Aliouane, L., 2015. Total organic carbon prediction in shale gas reservoirs from well logs data using the multilayer perceptron neural network with levenberg marquardt training algorithm: application to barnett shale. *Arabian J. Sci. Eng.* 40 (11), 3345–3349. <https://doi.org/10.1007/s13369-015-1685-y>.
- Parshall, J., 2015. Drilling data provide solution to horizontal well log costs. *J. Petrol. Technol.* 67 (8), 35–38.
- Pham, Nam, Wu, Ximeng, Naeini, Ehsan Zabihi, 2020. Missing well log prediction using convolutional long short-term memory network. *Jul Geophysics* 85 (Issue 4), 1JA-Z18.
- Povey, D., Hadian, H., Ghahremani, P., Li, K., Khudanpur, S., 2018. A time-restricted self-attention layer for ASR. In: IEEE International Conference on Acoustics, Speech and Signal Processing (ICASSP), Calgary, AB, 2018, pp. 5874–5878. <https://doi.org/10.1109/ICASSP.2018.8462497>.
- Rolon, L., Mohaghegh, S.D., Ameri, S., Gaskari, R., McDaniel, B., 2009. Using artificial neural networks to generate synthetic well logs. *Nov J. Nat. Gas Sci. Eng.* 1 (4–5), 118–133.
- Santoso, R., He, X., Hoteit, H., 2019. Application of machine-learning to construct simulation models from high-resolution fractured formation. In: Presented at Abu Dhabi International Petroleum Exhibition & Conference, Abu Dhabi, UAE, 11 - 14 November. SPE-197439-MS. <https://doi.org/10.2118/197439-MS>.
- Schuster, M., Paliwal, K.K., 1997. Bidirectional recurrent neural networks. *IEEE Trans. Signal Process.* 45, 2673–2681.
- Shen, Tao, Zhou, Tianyi, Long, Guodong, Jiang, Jing, Pan, Shirui, Zhang, Chengqi, 2017. Disan: directional self-attention network for rnn/cnn-free language understanding. CoRR, abs/1709. <http://arxiv.org/abs/1709.04696>.
- Vaswani, Ashish, Shazeer, Noam, Parmar, Niki, Uszkoreit, Jakob, Jones, Llion, Gomez, Aidan N., Kaiser, Lukasz, Polosukhin, Illia, 2017. Attention is all you need. *Advances in Neural Information Processing Systems*, pp. 6000–6010.
- Zang, Haixiang, Liu, Ling, Sun, Li, Cheng, Lilin, Wei, Zhinong, Sun, Guoqiang, 2020. Short-term global horizontal irradiance forecasting based on a hybrid CNN-LSTM model with spatiotemporal correlations. *Renew. Energy* 160, 26–41.
- Zhang, Dongxiao, Chen, Yuntian, Jin, Meng, 2018. Synthetic well logs generation via recurrent neural networks. *Petrol. Explor. Dev.* 45 (4), 69–79.